Redox Biology 22 (2019) 101145

Contents lists available at ScienceDirect

Redox Biology

journal homepage: www.elsevier.com/locate/redox

Research Paper

Systemic inactivation of hypoxia-inducible factor prolyl 4-hydroxylase 2 in mice protects from alcohol-induced fatty liver disease

Anna Laitakari[a], Teemu Ollonen[a], Thomas Kietzmann[b], Gail Walkinshaw[c], Daniela Mennerich[b], Valerio Izzi[a], Kirsi-Maria Haapasaari[d], Johanna Myllyharju[a], Raisa Serpi[a], Elitsa Y. Dimova[a], Peppi Koivunen[a,*]

[a] Biocenter Oulu, Faculty of Biochemistry and Molecular Medicine, Oulu Center for Cell-Matrix Research, University of Oulu, Oulu, Finland
[b] Faculty of Biochemistry and Molecular Medicine, University of Oulu, Oulu, Finland
[c] FibroGen Inc., San Francisco, CA, USA
[d] Department of Pathology, Medical Research Center Oulu, Oulu University Hospital and University of Oulu, Oulu, Finland

ARTICLE INFO

Keywords:
HIF
Hypoxia response
Inflammation
Metabolism
Oxidative stress

ABSTRACT

Alcoholic fatty liver disease (AFLD) is a growing health problem for which no targeted therapy is available. We set out to study whether systemic inactivation of the main hypoxia-inducible factor prolyl 4-hydroxylase, HIF-P4H-2 (PHD2/EglN1), whose inactivation has been associated with protection against metabolic dysfunction, could ameliorate it. HIF-P4H-2-deficient and wild-type (WT) mice or HIF-P4H inhibitor-treated WT mice were subjected to an ethanol diet for 3–4 weeks and their metabolic health, liver and white adipose tissue (WAT) were analyzed. Primary hepatocytes from the mice were used to study cellular ethanol metabolism. The HIF-P4H-2-deficient mice retained a healthier metabolic profile, including less adiposity, better lipoprotein profile and restored insulin sensitivity, while on the ethanol diet than the WT. They also demonstrated protection from alcohol-induced steatosis and liver damage and had less WAT inflammation. In liver and WAT the expression of the key lipogenic and adipocytokine mRNAs, such as *Fas* and *Ccl2*, were downregulated, respectively. The up-regulation of metabolic and antioxidant hypoxia-inducible factor (HIF) target genes, such as *Slcs 16a1* and *16a3* and *Gclc*, respectively, and a higher catalytic activity of ALDH2 in the HIF-P4H-2-deficient hepatocytes improved handling of the toxic ethanol metabolites and oxidative stress. Pharmacological HIF-P4H inhibition in the WT mice phenocopied the protection against AFLD. Our data show that global genetic inactivation of HIF-P4H-2 and pharmacological HIF-P4H inhibition can protect mice from alcohol-induced steatosis and liver injury, suggesting that HIF-P4H inhibitors, now in clinical trials for renal anemia, could also be studied in randomized clinical trials for treatment of AFLD.

Alcoholic fatty liver disease (AFLD), characterized by hepatic lipid accumulation following alcohol consumption, is the earliest stage of alcohol-induced liver disease [1,2]. It is reversible by refraining from alcohol consumption or keeping it moderate, but can also progress to alcoholic hepatitis, cirrhosis or hepatocellular carcinoma if alcohol consumption continues [1–3]. In liver ethanol is metabolized in hepatocytes mainly by alcohol dehydrogenase (ADH) to acetaldehyde, which is then converted to acetate by aldehyde dehydrogenase (ALDH). Both of these reactions reduce NAD^+ to NADH, resulting in an increased NADH/NAD^+ ratio, which leads to oxidative damage. Acetaldehyde is also highly toxic and can form harmful adducts with cellular biomolecules. The acetate generated is released from the liver and metabolized further to CO_2 or converted to acetyl-CoA in peripheral tissues and used for lipid and cholesterol biosynthesis. Alcohol increases peripheral lipolysis, and together with the altered hepatic redox potential and the rises in the supply of free fatty acids and glycerol (the substrates for triacylglycerol esterification), it results in fat accumulation in the liver. In addition to steatosis, reactive oxygen species (ROS) play a major role in alcohol-induced liver damage. Cytochrome P450 2E1 (CYP2E1), an alcohol-inducible enzyme which contributes to ethanol metabolism, uses oxygen for catalysis and oxidizes NADPH to $NADP^+$. This increases the amounts of ROS that can damage cell organelles and whose neutralization can deplete cellular antioxidant systems [4].

Decreased oxygen availability initiates the hypoxia response, a survival mechanism that has evolved to enable organisms to cope with

* Corresponding author. Faculty of Biochemistry and Molecular Medicine, University of Oulu, Aapistie 7C, FIN-90014 Oulu, Finland.
E-mail address: peppi.koivunen@oulu.fi (P. Koivunen).

https://doi.org/10.1016/j.redox.2019.101145
Received 22 December 2018; Received in revised form 6 February 2019; Accepted 14 February 2019
Available online 19 February 2019

low oxygen levels [5–7]. Hypoxia-inducible factors (HIFs), which consist of a labile α subunit and a stable β subunit, are the major governor of the transcriptional response initiated by hypoxia. When oxygen is available, three HIF prolyl 4-hydroxylases (HIF-P4Hs 1–3) target HIFα for proteasomal degradation via von Hippel Lindau protein (pVHL) [5]. HIF-P4H-2 (PHD2/EglN1) is the most abundant isoenzyme and the major one responsible for HIFα disruption [8]. It is also an essential gene, unlike *Hif-p4h-1* or *Hif-p4h-3*. [9–11] Under hypoxic conditions the catalytic activity of the highly oxygen-demanding HIF-P4Hs [12] is compromised, whereupon HIFα escapes degradation and forms a transcriptionally active αβ dimer that can bind to the hypoxia response elements in > 300 genes and upregulate their transcription. Many of these genes induce erythropoiesis and angiogenesis to increase oxygen availability and distribution, but a large number of HIF target genes also regulate energy metabolism to reduce the highly oxygen-demanding oxidative phosphorylation, and to induce non-oxygen-demanding glycolysis [5–7].

Hypoxia and HIF1α stabilization have been indicated following ethanol administration to the liver, however the contribution of HIF1α to AFLD is controversial [13]. No data are available on the role of any HIF-P4H in AFLD. It has been shown recently that systemic activation of the hypoxia response by inhibition of HIF-P4H-2, which stabilizes HIFα in several tissues in the presence of oxygen, protects mice from obesity and metabolic dysfunction including aging and high-fat-diet -induced steatosis [14]. This protection appeared to result from the HIF-mediated changes in gene expression that regulate lipid and glucose metabolism and is manifested in increased insulin sensitivity, for example [14]. We set out to study here whether chronic systemic inactivation of HIF-P4H-2 could protect mice from AFLD. Our data show that the *Hif-p4h-2* hypomorphic mice (*Hif-p4h-2*$^{gt/gt}$) retained a healthier metabolic profile and developed less steatosis and liver injury when on an ethanol diet than wild-type (WT) mice. Moreover, protection against liver injury was also observed when WT mice on an ethanol diet were treated with a pharmacological HIF-P4H inhibitor.

1. Materials and methods

1.1. Animal experiments

All the experiments were performed according to protocols approved by the National Animal Experiment Board of Finland, license numbers ESAVI-6154 and ESAVI-8179. *Hif-p4h-2*$^{gt/gt}$ mice were generated as previously described [15]. 4-month-old female *Hif-p4h-2*$^{gt/gt}$ mice were fed the Lieber-DeCarli liquid ethanol (5% v/v) diet or a control liquid diet (ethanol replaced with maltose-dextrin supplying equivalent calories) (F1258SP and F1259SP respectively, Bio-Serv) *ad libitum* for 3 weeks. Gender-matched WT littermates were used as controls. For the pharmacological study 1.5- year-old WT female mice were fed the Lieber-DeCarli liquid ethanol diet for 4 weeks and simultaneously given orally three times a week 60 mg/kg FG-4497 (HIF-P4H inhibitor, FibroGen Inc, USA), which was dissolved in 0.5% sodium carboxymethyl cellulose (Spectrum) and 0.1% polysorbate 80 (Fluka) [14]. The solvent was also used as a vehicle for the control group and administered orally three times per week.

1.2. Isolation and culture of primary hepatocytes

Primary hepatocytes were isolated from 12 to 14 week-old WT and *Hif-p4h-2*$^{gt/gt}$ mice fed normal chow by a standard two-step non-recirculating perfusion via the *vena cava*. In brief, the liver was perfused with a sterile carbogen-gassed Krebs-Ringer solution containing 0.25 mM EGTA to remove the blood completely. Thereafter, perfusion was continued with a buffer supplemented with 100 CDU/ml collagenase type II (Worthington) and 4 mM $CaCl_2$. The liver was dissected after removal and cells were separated from the debris through a 100 μm BD filter with washing buffer (20 mM HEPES, 120 mM NaCl, 4.8 mM KCl, 1.2 mM $MgSO_4$, 1.2 mM KH_2PO_4, 0.4% bovine serum albumin). Nonparenchymal cells and debris were separated from the hepatocytes by 4–5 centrifugations at 20 g for 3 min. Hepatocytes were cultured at +37 °C under 95% air/5% CO_2 in M199 (Lonza) containing 1% antibiotics, 10^{-9} M insulin (Sigma-Aldrich) and 10^{-7} M dexamethasone (Sigma-Aldrich). For the initial 4 h of culture 5% (v/v) fetal bovine serum (Biowest) was present. For experiments the hepatocytes were cultured in serum-free medium.

1.3. Cell culture

Hep3B cells (ATCC, HB-8064™) were cultured in MEM (Sigma-Aldrich) supplemented with 10% fetal bovine serum (Biowest), 1% nonessential amino acids (Sigma-Aldrich) and 1% antibiotics under standard conditions or exposed to 1% O_2 (hypoxia) in an InVivo2 400 hypoxia work station (Ruskinn Technologies).

1.4. Determination of serum alanine aminotransferase (ALT), acetate, lipids and insulin and blood glucose and ethanol levels

The baseline blood samples were taken 2 weeks prior to starting the control or ethanol diet. Serum was collected from the terminal blood of the mice at sacrifice. For the analysis of serum acetate at the 2-week time point of the ethanol diet, 20 μl of hind-limb venous blood was collected into a capillary. The isolated serum together with the baseline and sacrifice serum samples was analyzed with the acetate colorimetric assay kit (MAK086, Sigma-Aldrich). The ALT activity assay kit (MAK052, Sigma-Aldrich) was used to determine serum ALT levels. Serum total cholesterol, HDL cholesterol and triglyceride levels were determined by an enzymatic method (Roche Diagnostics), and LDL + VLDL cholesterol values were calculated using the Friedewald equation [16]. Serum insulin levels were determined with the Rat/Mouse Insulin ELISA kit (EZRMI-13 K, Millipore). Blood glucose concentrations were measured with a glucometer and the homeostatic model assessment-insulin resistance (HOMA-IR) index was calculated from the blood glucose and serum insulin values. Blood ethanol levels were determined with the Ethanol Assay Kit (Sigma Aldrich, MAK076-1KT) by a coupled enzyme reaction that results in a colorimetric product. The absorbances of the colorimetric products were determined with the Infinite M1000 Pro Multimode Plate Reader (Tecan).

1.5. Histological analyses

Five-micrometer sections from frozen cryo-sectioned liver samples were stained with Oil Red O (ORO) (O0625; Sigma-Aldrich) and formalin-fixed paraffin-embedded liver and white adipose tissue (WAT) samples were stained with hematoxylin-eosin (H&E). All these were viewed with a Leica DM LB2 microscope and photographed with a Leica DFC 320 camera. Hepatic steatosis in the H&E and ORO-stained sections was scored (0–4 +). Representative images of WAT tissue (5–8 per mouse) were taken and the areas of 100 adipocytes were quantified with the Adobe Photoshop CS5 Magnetic Lasso Tool. Infiltration of CD68-positive macrophages into WAT was quantified with an anti-CD68 antibody (ab955; Abcam) in five fields per sample. Liver pericentral zonation was evaluated with an anti-glutamine synthetase (GS) antibody (610518; clone 6; BD Biosciences). Quantification of the GS-positive staining zone in ethanol-fed livers was done by measuring the width of this layer of five pericentral zones per mouse with Adobe Photoshop. Liver inflammation and necrosis were scored from the H&E stained sections. Necrosis and inflammation were scored 0–4 as: 0 = “None”, 1 = “Mild”, 2 = “Moderate”, 3–4 = “Severe”. To analyze the level of apoptosis, liver samples were stained with the In Situ Cell Death Detection kit, fluorescein (Roche), and the number of apoptotic cells or bodies was calculated from 5 to 8 fields per mouse using an Olympus BX21 microscope and an Olympus XC50 camera. Liver mitotic cells were calculated from 10 fields per mouse using an Olympus BX21

microscope and an Olympus XC50 camera from the H&E stained sections. Liver fibrosis was determined by Masson's Trichrome staining of the formalin-fixed paraffin-embedded samples.

1.6. Quantitative real-time PCR (qPCR) analyses

Total RNA was isolated from the cells and liver and WAT tissues with E.Z.N.A. Total RNA Kit II (Omega Bio-Tek) or with TriPure Isolation Reagent (Roche Applied Science) purified with E.Z.N.A. Total RNA Kit I (Omega Bio-Tek) and reverse transcribed with an iScript cDNA Synthesis Kit (Bio-Rad). qPCR was performed with iTaq SYBR Green Supermix with ROX (Bio-Rad) in a C1000 Touch Thermal Cycler and a CFX96 Touch Real-Time PCR Detection System (Bio-Rad) with the primers shown in Supplementary Table 1.

1.7. Western blot analyses of tissue and cells

Dissected livers were snap-frozen in liquid nitrogen and protein lysates for the detection of HIF1α and HIF2α proteins were extracted with the NE-PER kit (Pierce). Primary hepatocytes and Hep3B cells were lysed in buffer of 50 mM Tris–HCl, pH 8, 150 mM NaCl, 0.5% NP-40, 1 mM PMSF and a complete protease inhibitor cocktail tablet (Roche), kept on ice for 20 min and centrifuged at 12 000 g for 20 min at 4 °C. 100 μg of proteins from liver or cells were resolved by SDS-PAGE, blotted, and probed with the following primary antibodies: HIF1α (NB-100479, Novus Biologicals), HIF2α (NB100-122, Novus Biologicals) and β-actin (NB600-501, clone AC-15, Novus Biologicals). The secondary antibody, either anti-mouse or anti-rabbit, was conjugated to horseradish peroxidase (1:5000; Bio-Rad Laboratories). The Pierce ECL system (ThermoScientific) was used for detection.

1.8. Determination of triglycerides in liver tissue and primary hepatocytes

Hepatic lipids were extracted by overnight digestion in an ethanol-KOH-solution at +55 °C followed by centrifugation at 10 000 g for 5 min. The lipids in the supernatant were precipitated on ice with $MgCl_2$. After a second centrifugation at 10 000 g for 5 min the supernatant was assayed for triglycerides by an enzymatic method (Roche Diagnostics) and the absorbances of the colorimetric products were determined with the Infinite M1000 Pro Multimode Plate Reader (Tecan). Primary hepatocytes from WT and *Hif-p4h-2*$^{gt/gt}$ mice were treated with 0.5 mM NAC, 100 mM EtOH or combination of both for 72 h. In the latter case, cells were pretreated with 0.5 mM NAC for 1 h before the EtOH challenge. The dose of NAC and/or EtOH was added each day with a fresh medium to maintain the NAC and/or EtOH at a constant level. Triglyceride content was measured in the cell extracts of 1×10^6 viable cells using Triglyceride quantification kit (MAK266, Sigma-Aldrich) according to the manufacturer's instructions.

1.9. ROS measurements

Intracellular ROS in the primary hepatocytes were assessed using the fluorescence based CellRox™ (ThermoFischer Scientific) method. Fluorescence was recorded in the Infinite M1000 Pro Multimode microplate reader (Tecan). Dead cells were assessed by staining with SYTOX™ (ThermoFischer Scientific) according to the manufacturer's instructions and eliminated from the calculations of ROS levels.

1.10. Aldehyde dehydrogenase 2 (ALDH2) activity assay

The activity of ALDH2 was determined using the ALDH2 activity assay kit according to the manufacturer's protocol (ab115348, Abcam).

1.11. Reduced glutathione (GSH) assay

GSH levels were measured using *o*-phthaldialdehyde as a fluorescent agent [17] as described [18].

1.12. Statistical analyses

Power calculations were carried out prior to experiments to use the smallest possible number of animals to obtain significant data. Student's two-tailed *t*-test was used for the statistical significance of differences between two groups and Fisher's exact test for data based on histological scoring. To compare linear dependences between two variables, Pearson's correlation coefficient was used. All data are presented as means ± standard error of the mean (SEM) unless otherwise stated. $p \leq 0.05$ was considered statistically significant.

2. Results

2.1. HIF-P4H-2-deficient mice retained a healthier metabolic profile on the ethanol diet

Hif-p4h-2$^{gt/gt}$ female mice and their WT littermates were fed the Lieber-DeCarli liquid diet supplemented with 5% (v/v) ethanol (ethanol diet) or equal calories (control diet) for three weeks. There was no difference in the daily food intake between the genotypes (Supporting Fig. S1A) and the plasma ethanol concentration of all the mice fed the ethanol diet was about 60 mg/dl at three weeks (Supporting Fig. S1B). The *Hif-p4h-2*$^{gt/gt}$ mice retained a ~15% lower body weight on both diets than the WT (Fig. 1A). In agreement with the established lipolytic effect of ethanol [19], the ethanol diet reduced the amount of gonadal WAT and significantly reduced the size of the adipocytes in both genotypes compared with the control diet (Fig. 1B and C). However, the *Hif-p4h-2*$^{gt/gt}$ mice had less WAT and smaller adipocytes than the WT on both diets (Fig. 1B and C). The *Hif-p4h-2*$^{gt/gt}$ mice had lower serum total cholesterol levels than the WT on both the control and ethanol diet (Fig. 1D). The ethanol diet significantly increased serum HDL levels in the *Hif-p4h-2*$^{gt/gt}$ mice (from 1.4 ± 0.3 mmol/l to 2.1 ± 0.2 mmol/l, $p < 0.05$) and they had a higher HDL/LDL + VLDL ratio on this diet compared with WT (Fig. 1D). The ethanol diet also increased the serum triglyceride levels almost two-fold in both genotypes relative to the control diet, but no difference was detected between the groups on either diet (Fig. 1D). Additionally, the ethanol diet increased blood glucose and serum insulin levels and the HOMA-IR score in the WT but not the *Hif-p4h-2*$^{gt/gt}$ mice, the latter having significantly lower glucose and HOMA-IR values on the ethanol diet compared with the WT (Fig. 1E,F,G).

2.2. HIF-P4H-2 deficiency provided protection from alcohol-induced steatosis and liver damage

The 3-week ethanol diet increased significantly the liver weights compared with the control diet in both genotypes, however the increase in the *Hif-p4h-2*$^{gt/gt}$ mice was only 20% whereas it was 40% in the WT (Fig. 2A). The liver weights of the WT mice on the ethanol diet were 22% higher than those of the *Hif-p4h-2*$^{gt/gt}$ mice (Fig. 2A). Also, in the WT mice the ethanol diet significantly increased the amount of microvesicular hepatic steatosis compared with the control diet, whereas no such significant increase was seen in the *Hif-p4h-2*$^{gt/gt}$ mice, which had lower steatosis scores than the WT mice on both diets (Fig. 2B). In agreement with the histological data, the amount of triglycerides in the alcohol-fed WT livers was significantly higher than in the control diet livers, whereas the increase in the *Hif-p4h-2*$^{gt/gt}$ mice was not significant ($p = 0.065$, Fig. 2C), and the triglyceride content on the ethanol diet in WT was > 150% of that in the *Hif-p4h-2*$^{gt/gt}$ livers (Fig. 2C). There was a significant positive correlation ($r = 0.646$, $p = 0.00006$) between the steatosis scores and hepatic triglycerides. Furthermore, the ethanol diet increased significantly serum ALT levels in the WT but not *Hif-p4h-2*$^{gt/gt}$ mice ($p = 0.070$, Fig. 2D). The WT mice also had significantly higher serum ALT levels on the ethanol diet than the *Hif-p4h-2*$^{gt/gt}$ mice

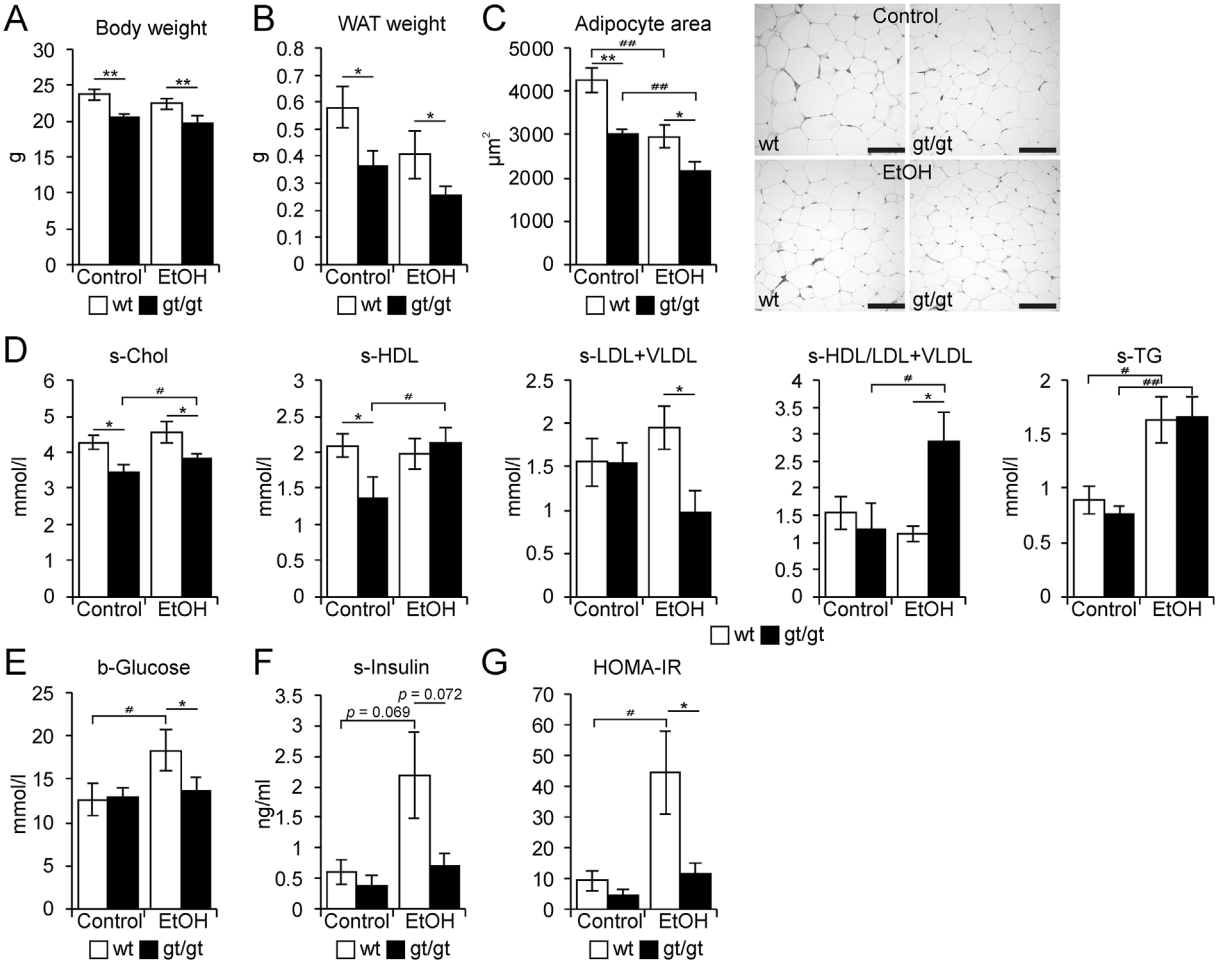

Fig. 1. HIF-P4H-2-deficient mice retain a healthier metabolic profile on an ethanol diet. Wild-type (wt) and *Hif-p4h-2*$^{gt/gt}$ (gt/gt) mice after the administration of an ethanol (EtOH) or control diet for 3 weeks (n = 7–10/group). (A) Body weight of wt and gt/gt mice. (B) Weight of gonadal WAT. (C) Cross-sectional area of WAT adipocytes. Scale bar = 100 µm. (D) Serum total cholesterol, HDL cholesterol, LDL + VLDL cholesterol and HDL/LDL + VLDL cholesterol ratios, TG levels. (E) Blood glucose values. (F) Serum insulin values. (G) HOMA-IR scores. Data are means ± SEM. * or #$p \leq 0.05$, ** or ##$p < 0.01$. Abbreviations: b, blood; s, serum; TG, triglycerides; WAT, white adipose tissue.

(Fig. 2D) indicating less liver damage in the latter. Since the pericentral zonation marker glutamine synthetase (GS) is generally considered to be a marker of liver integrity [18] we performed respective immunohistochemical stainings. In line with the serum parameters, the analyses of the liver sections revealed an impaired acinar integrity as indicated by a less stringent pericentral zonation, appearance of more dispersed GS-positive hepatocytes as well as a generally stronger GS expression in the alcohol-fed WT livers compared with the control diet-fed livers or the ethanol-fed *Hif-p4h-2*$^{gt/gt}$ livers (Fig. 2E). Quantification of the width of the GS expression layer revealed that it was about 10% wider in the alcohol-fed WT livers compared with the *Hif-p4h-2*$^{gt/gt}$ but the difference did not reach significance (69.4 ± 10.5 µm in WT vs. 64.0 ± 15.7 µm in *Hif-p4h-2*$^{gt/gt}$). Altogether, this suggests better preserved liver function in the *Hif-p4h-2*$^{gt/gt}$ livers on the ethanol diet. The ethanol diet did not induce significant hepatic inflammation, fibrosis or necrosis and no difference in liver apoptosis or regeneration was detected between the genotypes (Supporting Fig. S2A,B,C,D,E).

2.3. Changes in mRNA expression levels in liver and WAT associated with protection from steatosis in the HIF-P4H-2 deficient mice

We next studied the expression levels of the key lipogenic mRNAs, sterol regulatory element binding transcription factor 1c (*Srebf1c*), fatty acid synthase (*Fas*) and stearoyl-CoA desaturase 1 (*Scd1*), and found that the level of *Fas* became significantly upregulated on the ethanol diet compared with the control diet in both genotypes, but its level in the *Hif-p4h-2*$^{gt/gt}$ livers was yet significantly lower (Fig. 3A). In WT livers *Scd* mRNA levels almost quadrupled on the ethanol diet compared with the control diet while no significant increase was observed in the *Hif-p4h-2*$^{gt/gt}$ livers that had significantly lower levels of it on ethanol diet (Fig. 3A). We also found decreased expression of catenin beta 1 (*Ctnnb1*) mRNA, a regulator of GS expression, in the *Hif-p4h-2*$^{gt/gt}$ livers on the ethanol diet as compared with the WT (Fig. 3A), these data being in agreement with the immunohistochemical staining for GS (Fig. 2E). The mRNA expression levels of *Ctnnb1* correlated positively with serum ALT levels (Fig. 3B), agreeing with the β-catenin pathway disruption being associated with the pathogenesis of AFLD [20]. The mRNA level of the inflammatory C-C motif chemokine ligand 2 (*Ccl2*) increased by 7-fold on the ethanol diet in WT WAT while the increase was 3-fold in the *Hif-p4h-2*$^{gt/gt}$ WAT which had significantly lower *Ccl2* levels on both diets (Fig. 3C). The mRNA levels of the central energy homeostasis and appetite regulator leptin (*Lep*) were significantly lower in the *Hif-p4h-2*$^{gt/gt}$ WAT as compared with the WT on the ethanol diet (Fig. 3C). These were accompanied by reduced accumulation of the inflammatory WAT macrophages (Fig. 3D). The expression level of the adipose *Lep* mRNA correlated positively with the number of the WAT macrophages (Fig. 3E).

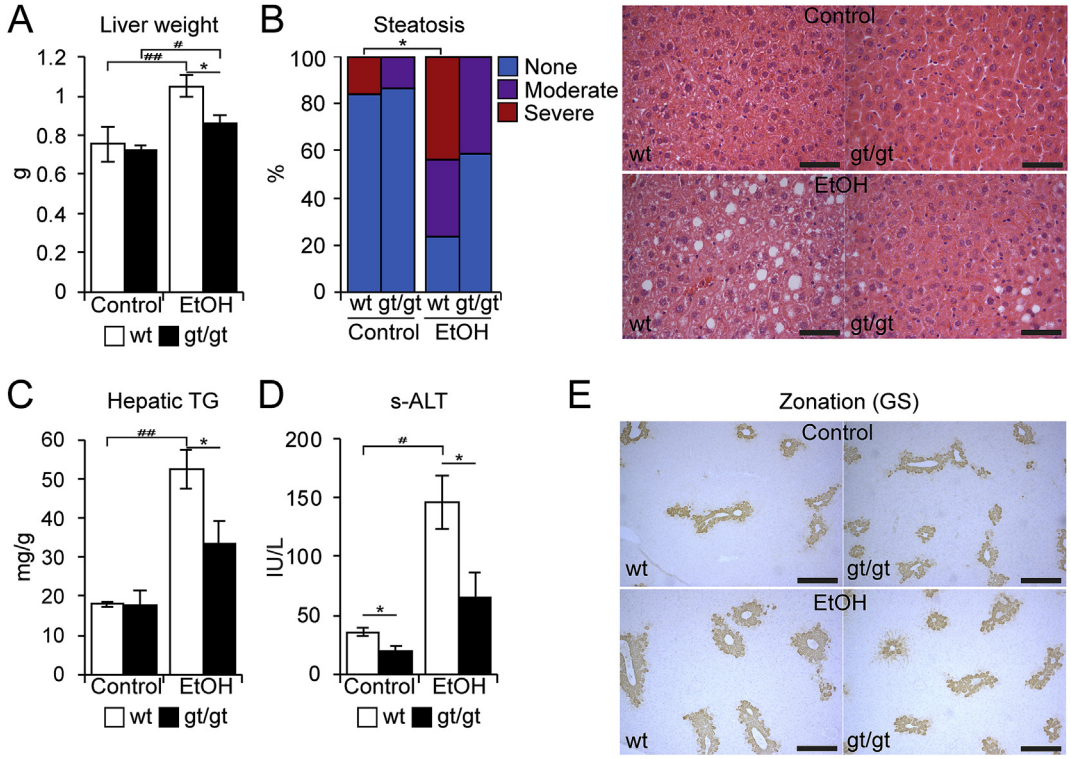

Fig. 2. HIF-P4H-2 deficiency protects mice from alcoholic fatty liver disease. Wild-type (wt) and *Hif-p4h-2*$^{gt/gt}$ (gt/gt) mice after the administration of an ethanol (EtOH) or control diet for 3 weeks (n = 6–10/group). (A) Liver weight. (B) Scoring of steatosis from ORO-stained samples. H&E-stained liver sections. Scale bar = 50 μm. (C) Hepatic TG content. (D) Serum ALT levels. (E) GS-stained liver sections showing liver pericentral zones. Scale bar = 200 μm. Data are means ± SEM. For grading of steatosis scores 0–2 correspond to "None", 3 to "Moderate" and 4 to "Severe". * or #$p < 0.05$, ##$p < 0.01$. Abbreviations: ALT, alanine aminotransferase; GS, glutamine synthetase; ORO, Oil Red O; s, serum; TG, triglycerides. (For interpretation of the references to color in this figure legend, the reader is referred to the Web version of this article.)

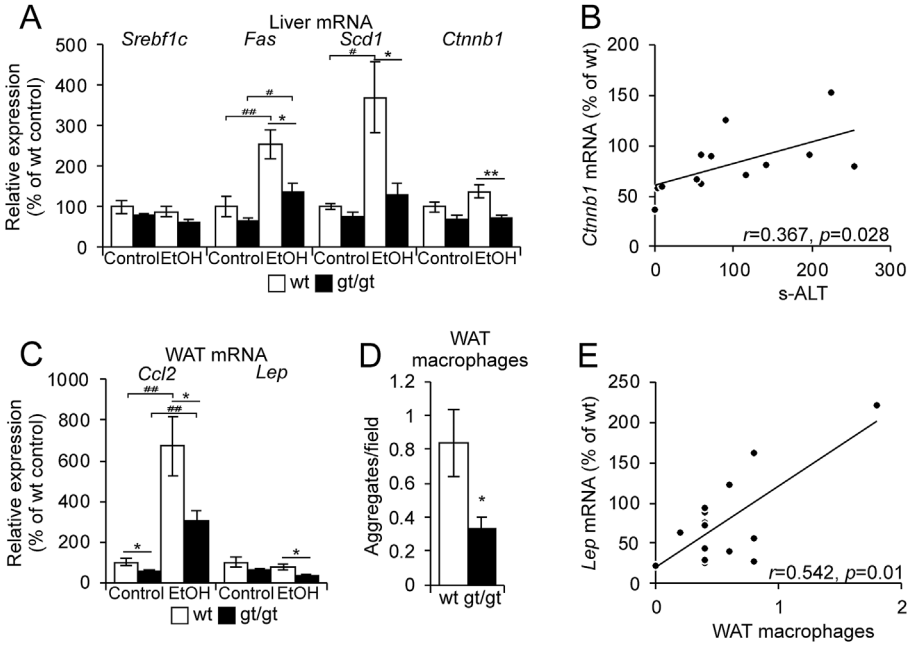

Fig. 3. Changes in hepatic and adipose mRNA expression levels associated with protection from steatosis in the HIF-P4H-2-deficient mice on the ethanol diet. Wild-type (wt) and *Hif-p4h-2*$^{gt/gt}$ (gt/gt) mice after the administration of an ethanol diet for 3 weeks (n = 6–10/group). (A, C) qPCR analysis of the mRNA levels of the indicated genes in the liver (A) and WAT (C) of gt/gt and wt mice on control diet or ethanol (EtOH) diet. The expression of each gene was studied relative to TATA-box binding protein mRNA in the liver and to peptidylprolyl isomerase A mRNA in WAT. (B) Correlation of hepatic *Ctnnb1* mRNA levels with s-ALT levels. (D) Number of macrophage aggregates in gonadal WAT. (E) Correlation of WAT leptin mRNA levels with WAT macrophage aggregate numbers. Data are means ± SEM. *$p < 0.05$, **$p < 0.01$. Abbreviations: *Ccl2*, C-C motif chemokine ligand 2; *Ctnnb1*, catenin beta 1; *Fas*, fatty acid synthase; *Lep*, leptin; qPCR, quantitative real time PCR; *Scd1*, stearoyl-CoA desaturase 1; s, serum; *Srebf1c*, sterol regulatory element binding transcription factor 1c; WAT, white adipose tissue.

2.4. HIF-P4H-2 deficient mice were better at handling the toxic metabolites of ethanol and oxidative stress

Although there was no difference in plasma ethanol levels between the WT and *Hif-p4h-2*$^{gt/gt}$ mice (Supporting Fig. S1B), the serum acetate levels were significantly higher in the latter on the ethanol diet (Fig. 4A). This suggested an alteration in the rate of ethanol metabolism in the *Hif-p4h-2*$^{gt/gt}$ mice. We therefore isolated primary hepatocytes from the mice at baseline and first analyzed the expression of the key ethanol metabolizing enzymes. These analyses indicated no difference in *Adh1* or *Aldh2* mRNA levels between the genotypes (Fig. 4B). Since acetate is primarily the product of ALDH2 we next measured ALDH2

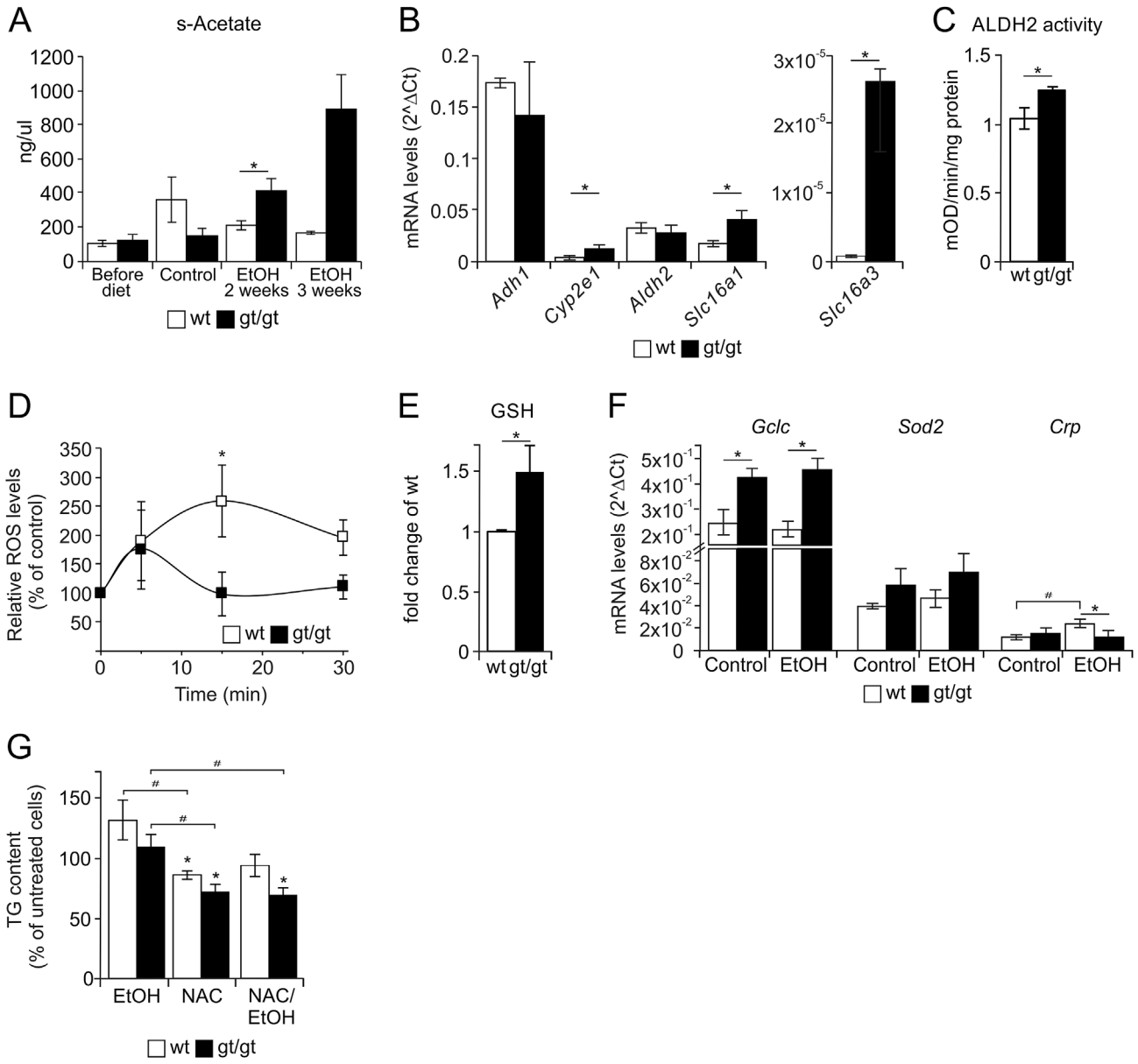

Fig. 4. Altered ethanol metabolism and oxygen radical scavenging in HIF-P4H-2-deficient mice and hepatocytes. (A) Serum acetate levels of wild-type (wt) and *Hif-p4h-2*$^{gt/gt}$ (gt/gt) mice before and after the administration of a control diet for 3 weeks (n = 8/group for both) or an ethanol (EtOH) diet for 2 (n = 5/group) and 3 weeks (pooled samples, n = 6/group). (B–G) Primary hepatocytes were isolated from mice fed normal chow. (B) qPCR analysis of wt and gt/gt hepatocytes. mRNA levels were normalized to the levels of actin beta mRNA (n = 3–4/group). (C) *In vitro* ALDH2 enzymatic activity in wt and gt/gt hepatocytes (n = 3/group). (D) The redox state of hepatocytes treated with 100 mM EtOH and followed for 30 min was determined by measuring CellRox fluorescence. The data were calculated as percentages of the control (untreated) (n = 4–5/group). (E) Reduced glutathione (GSH) levels in wt and gt/gt hepatocytes, normalized to wt (n = 3/group). (F) qPCR analysis of hepatocytes following control or 100 mM ethanol treatment for 24 h (n = 4/group). (G) Triglyceride determination from wt and gt/gt hepatocytes exposed to 0.5 mM NAC, 100 mM EtOH or combination of both for 72 h. Data are expressed as percentage of triglycerides relative to untreated cells (n = 3/group). * = treatment vs. control (untreated cells). Data are means ± SEM. * or #$p \leq 0.05$. The statistical significance for (A) 3-week time point could not be tested due to use of pooled samples. *p* values in (B) were calculated from the log-transformed values. Abbreviations: *Adh1*, alcohol dehydrogenase 1A; *Crp*, C-reactive protein; *Cyp2e1*, cytochrome P450 2E1; *Aldh2,* aldehyde dehydrogenase 2; *Gclc*, glutamate-cysteine ligase catalytic subunit; NAC, N-acetyl cysteine; *Slc16a1* and *Slc16a3*, solute carrier family 16, members 1 and 3; *Sod2*, superoxide dismutase 2; TG, triglyceride.

activity in primary hepatocytes and found it to be 25% higher in the *Hif-p4h-2*$^{gt/gt}$ cells than the WT (Fig. 4C). The increased ALDH2 activity in the *Hif-p4h-2*$^{gt/gt}$ hepatocytes was in line with the detected enhanced mRNA expression of the monocarboxylate transporters solute carrier family 16 members 1 and 3 (*Slc16a1* and *Slc16a3*) which are involved in acetate transport (Fig. 4B). Moreover, *Cyp2e1* mRNA was significantly upregulated in the *Hif-p4h-2*$^{gt/gt}$ hepatocytes compared with the WT (Fig. 4B). Since the activity of CYP2E1 is connected to ROS production, we next investigated whether the *Hif-p4h-2*$^{gt/gt}$ hepatocytes would be better equipped against harmful ROS effects. To do this, we treated WT and *Hif-p4h-2*$^{gt/gt}$ hepatocytes with 100 mM ethanol and measured ROS levels over time. We found that ethanol mediated a transient induction of ROS formation (Fig. 4D). The WT hepatocytes displayed a robust formation of ROS with a maximal induction of about 2.5-fold after 15 min, thereafter the ROS levels declined (Fig. 4D). By contrast, the response in the *Hif-p4h-2*$^{gt/gt}$ hepatocytes was much less pronounced, the maximal induction of about 1.5-fold was already reached 5 min after treatment with ethanol (Fig. 4D). Thus, it appears that the *Hif-p4h-2*$^{gt/gt}$ hepatocytes had the ability to clear ROS significantly faster than the WT (Fig. 4D). Indeed, we detected higher

levels of the ROS scavenging reduced glutathione (GSH) in the baseline *Hif-p4h-2*$^{gt/gt}$ hepatocytes compared with the WT (Fig. 4E), and the upregulation of the GSH synthesizing glutathione cysteine ligase (*Glcl*) mRNA expression following control or ethanol treatment, corroborated the observed effects (Fig. 4F). Moreover, the mRNA for another ROS scavenging enzyme, superoxide dismutase 2 (*Sod2*), was stronger expressed in the *Hif-p4h-2*$^{gt/gt}$ hepatocytes following control or ethanol treatment compared with the WT (Fig. 4F). Interestingly, ethanol treatment significantly increased the C-reactive protein (*Crp*) mRNA levels only in the WT but not the *Hif-p4h-2*$^{gt/gt}$ hepatocytes, its levels being twice as high in the WT than in the *Hif-p4h-2*-deficient cells following ethanol treatment (Fig. 4F). Altogether, the *Hif-p4h-2*-deficient hepatocytes possessed a higher capacity to cope with ethanol-induced ROS formation. Additionally, the hepatocytes exposed to ethanol showed a trend to increased triglyceride content, especially in the WT (Fig. 4G). Treatment of the cells with a ROS scavenger N-acetyl cysteine (NAC) alone reduced the triglyceride levels in both genotypes and combination of NAC and EtOH significantly inhibited triglyceride accumulation in the *Hif-p4h-2*-deficient hepatocytes (Fig. 4G). Thus, these data imply that the enhanced antioxidant system in the *Hif-p4h-2*-deficient hepatocytes could have contributed to the observed attenuation of the liver fat accumulation *in vivo*.

Since ethanol has been reported to stabilize HIF, we analyzed the status of HIF1α and HIF2α in WT primary hepatocytes following ethanol treatment. Hydrogen peroxide (H_2O_2) and *t*-butyl hydroperoxide (TBH) were used as positive controls for ROS generation, and hypoxia (1% O_2) and HIF-P4H inhibitor (FG-4497) treatment as positive controls for HIF stabilization. Our data indicated that neither HIF1α nor HIF2α became stabilized in the hepatocytes following ethanol treatment (Supporting Fig. S3A), nor did ethanol stabilize HIFαs in Hep3B cells (Supporting Fig. S3B). Although H_2O_2 and TBH did not stabilize HIFαs in the primary hepatocytes, they did stabilize HIF1α in Hep3B cells (Supporting Figs. S3A and B). These data would suggest that the earlier reported HIF stabilization was not a direct effect of ethanol metabolism in primary hepatocytes [21,22].

2.5. Pharmacological HIF-P4H inhibition protected the WT mice from AFLD

Finally, we fed female WT mice an ethanol diet (5% v/v) for four weeks and treated them simultaneously three times a week with a preclinical pharmacological pan HIF-P4H inhibitor FG-4497 (60 mg/kg) or with vehicle alone. As expected, FG-4497 stabilized HIF1α and HIF2α in the liver (Fig. 5A) and upregulated the mRNAs of HIF target genes including *Hif-p4h-2* and several glycolytic enzymes (Supporting Fig. S4). In agreement with the earlier shown improved glucose tolerance following global activation of the hypoxia response [14], the glucose-regulated glucose transporter 2 (*Glut2*) mRNA was downregulated (Supporting Fig. S4). After four weeks on the diet 60% of the vehicle but only 20% of the FG-4497-treated mice had macrovesicular steatosis (Fig. 5B). The amount of microvesicular steatosis was also lower in the FG-4497-treated mice than in the vehicle-treated ones (Fig. 5C), as was the level of serum ALT (Fig. 5D). The HOMA-IR scores, WAT weight, adipocyte area and the number of the inflammatory WAT macrophage aggregates were also lower in the FG-4497-treated mice (Fig. 5E, F, G, H), and these mice similarly had lower serum total cholesterol, HDL and LDL + VLDL levels and a higher HDL/LDL + VLDL ratio compared with the vehicle (Fig. 5I). Likewise the lipogenic mRNAs were significantly downregulated in the liver of the FG-4497-treated mice by comparison with the vehicle-treated ones (Fig. 5J) and *Ccl2* and *Lep* mRNAs were downregulated in WAT (Fig. 5K). There were significant positive correlations between the serum ALT levels and the hepatic lipogenic mRNAs, *Srebf1c* ($r = 0.534$, $p = 0.01$), acetyl-CoA carboxylase α (*Acca*) (Fig. 5L), *Fas* ($r = 0.694$, $p = 0.001$) and *Scd1* ($r = 0.590$, $p = 0.009$), respectively, and also between the adipose tissue *Ccl2* mRNA levels and serum ALT levels (Fig. 5M), associating the reduced WAT inflammation with protection against liver damage and underlining the interplay between tissues in the disease mechanism. Altogether, these data suggest that pharmacological inhibition of HIF prolyl hydroxylases that activates the endogenous hypoxia response, offered a protective effect against AFLD.

3. Discussion

Chronic alcohol consumption negatively affects many tissues, the central finding being a fatty liver that can lead to inflammatory hepatosteatosis, irreversible cirrhosis and hepatocellular carcinoma. Excessive alcohol consumption also increases the risk of hypertriglyceridemia, hypertension, type 2 diabetes, pancreatitis and cardiomyopathy. Our data suggest that chronic global pharmacological inhibition of HIF-P4Hs is protective against alcohol-induced steatosis and liver damage in mice (Fig. 6). Since the same beneficial effects were also seen in mice with only genetic HIF-P4H-2 inactivation (Fig. 6), it is likely that the protection offered by FG-4497 treatment against AFLD was mediated by HIF-P4H-2 inhibition. The mechanisms involved included an overall improved metabolic profile with less steatosis and adiposity, protection against dyslipidemia and better insulin sensitivity, and faster clearance of the toxic ethanol metabolites, such as acetaldehyde and ROS, and provided evidence of an interplay between tissues (Fig. 6).

Inactivation of pVHL, but not HIF-P4H-2, in the mouse liver causes hepatomegaly and hepatic steatosis [11,23], and the combination of *Cre-ER* conditional *Hif-p4h-2* knockout and *Hif-p4h-3*$^{-/-}$ has been reported to induce hepatic steatosis in mice on normal chow [24]. Constitutive activation of HIF2α in the adult mouse liver has been shown to contribute to severe steatosis associated with impaired fatty acid β-oxidation, decreased lipogenic gene expression and increased lipid storage capacity [25]. HIF2α has also been suggested recently as a therapeutic target for non-alcoholic fatty liver disease (NAFLD) functioning via an intestinal HIF2α-NEU3 pathway that controls serum ceramide levels and affects NAFLD development [26]. We have reported earlier that *Hif-p4h-2*$^{gt/gt}$ mice who have normoxic stabilization of HIF2α in the liver and upregulation of the insulin sensitivity-increasing insulin receptor substrate 2 (*Irs2*) mRNA as well as downregulation of the lipogenic *Srebf1c, Fas, Acca* and *Scd* mRNAs [14,15], had less hepatic acetyl-CoA and a lower rate of *de novo lipogenesis* in the liver when on normal chow [14]. The data presented here show that these mice could additionally resist alcohol-induced steatosis and liver damage, as could WT mice fed a pharmacological HIF-P4H inhibitor, as exemplified by the reduced hepatic *Acca* mRNA level associated with the lower serum ALT levels (Fig. 6). Interestingly, the data observed in the primary hepatocytes suggest that the observed improved antioxidant capacity in the *Hif-p4h-2*$^{gt/gt}$ cells partly contributes to less stored triglycerides in liver in addition to improved clearance of the toxic metabolites of ethanol. Our data also suggest that it is important to have a systemic inactivation of the HIF P4Hs to obtain these beneficial metabolic effects rather than a cell type-specific HIFα activation, which can, on the contrary, be harmful [21,25,26]. This will contribute to the HIF-driven metabolic reprogramming that manifests itself in overall improved glucose tolerance, insulin sensitivity, an improved serum lipid profile and reduced adiposity and adipose tissue inflammation [14]. Our data likewise suggest that the dosage of the HIF-P4H-2 inhibitor is of importance. The hypomorphs have a 40% knockdown of *Hif-p4h*-2 mRNA in the liver, with the knockdown level in other tissues varying from > 90% in the heart to 80% in skeletal muscle, 50% in WAT and 40% in the brain [14,15,27]. To avoid the potentially negative effects of a full-powered HIF response, FG-4497 was administered three times a week. It appears that the endogenous feedback mechanism built into the hypoxia response, which is mediated at least partly by the HIF-inducible HIF-P4H-3 [24], is of great importance in keeping the HIF response in the physiological range. This feedback is compromised when HIF2α is constitutively active [25], and the levels of it are typically many fold higher than those received by

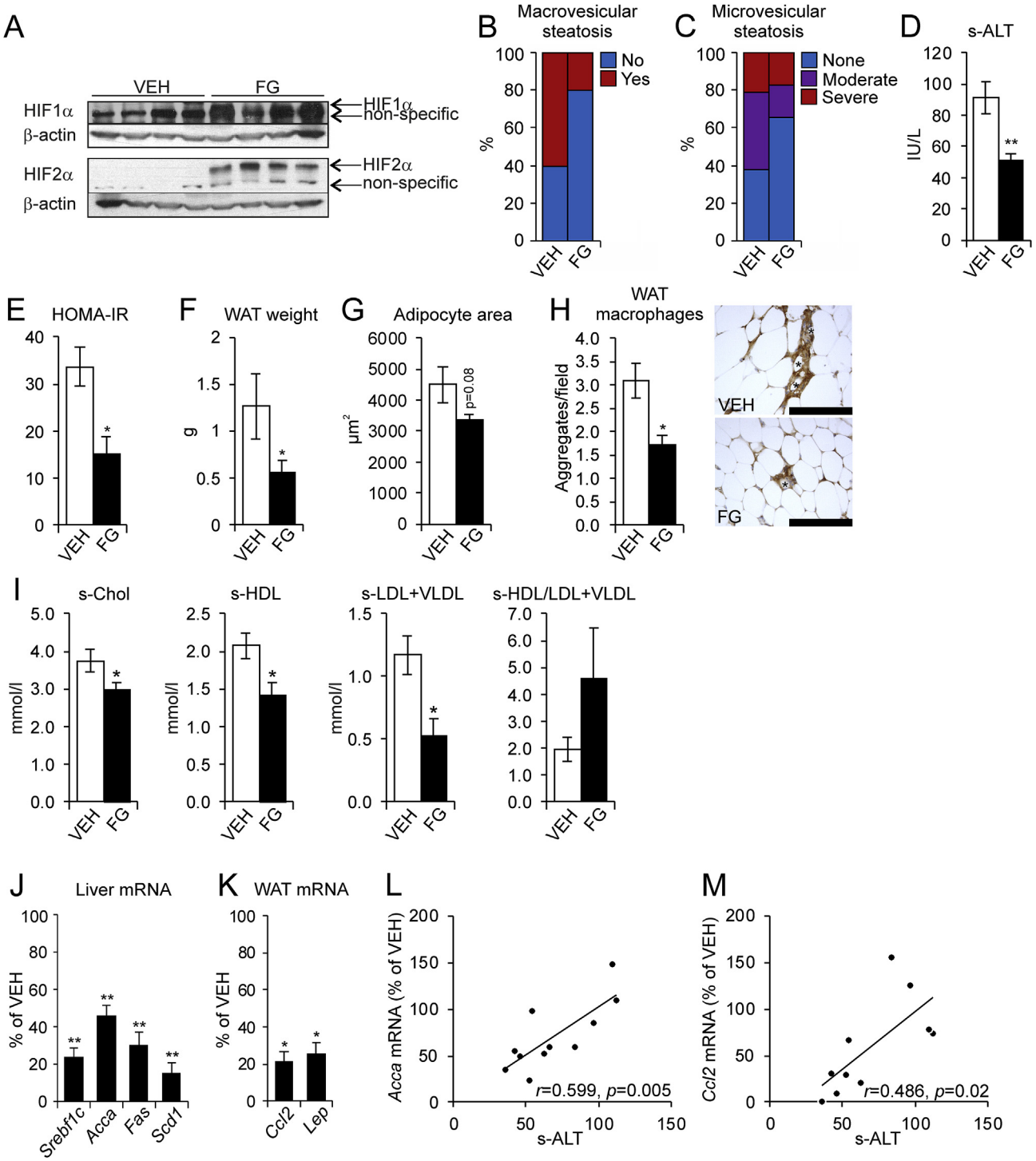

Fig. 5. Pharmacological inhibition of HIF-P4Hs protects mice from alcohol-induced metabolic dysfunction and liver damage. Wild-type mice were fed the ethanol diet for 4 weeks and simultaneously given vehicle (VEH) or 60 mg/kg of FG-4497 (FG) on days 1, 3 and 5 of each week (n = 4–6/group). (A) Western blot analysis of liver HIF1α and HIF2α protein levels from vehicle and FG-4497-treated mice. β-actin was used as a loading control. (B) Scoring of macrovesicular steatosis from hematoxylin&eosin-stained liver sections. For steatosis grading scores 0–2 correspond to "No" and 3–4 to "Yes". (C) Scoring of microvesicular steatosis from ORO-stained liver sections. For steatosis grading scores 0–2 correspond to "None", 3 to "Moderate" and 4 to "Severe". (D) Serum ALT levels. (E) HOMA-IR scores. (F) Weight of gonadal WAT. (G) Cross-sectional area of WAT adipocytes. (H) Number of macrophage aggregates in gonadal WAT. (*) = Adipocytes surrounded by macrophage aggregates. Scale bar = 100 μm (n = 3–4/group). (I) Serum total cholesterol, HDL cholesterol, LDL + VLDL cholesterol and HDL/LDL + VLDL cholesterol ratio. (J, K) qPCR analysis of mRNA levels of the indicated genes in the liver (J) and WAT (K) of FG-4497-treated mice relative to the vehicle. The expression of each gene was studied relative to TATA-box binding protein mRNA in the liver and to peptidylprolyl isomerase A mRNA in WAT. (L) Correlation of hepatic *Acca* mRNA levels with s-ALT levels. (M) Correlation of adipose tissue *Ccl2* mRNA levels with s-ALT levels. Data are means ± SEM. $*p \leq 0.05$, $**p < 0.01$. The *p* value for *Lep* in (K) was calculated from log-transformed values. Abbreviations: *Acca*, Acetyl-CoA carboxylase alpha; ALT, alanine aminotransferase; *Ccl2*, C-C motif chemokine ligand 2; *Fas*, fatty acid synthase; *Lep*, leptin; ORO, Oil Red O; *Scd1*, stearoyl-CoA desaturase 1; s, serum; *Srebf1c*, sterol regulatory element binding transcription factor 1c. (For interpretation of the references to color in this figure legend, the reader is referred to the Web version of this article.)

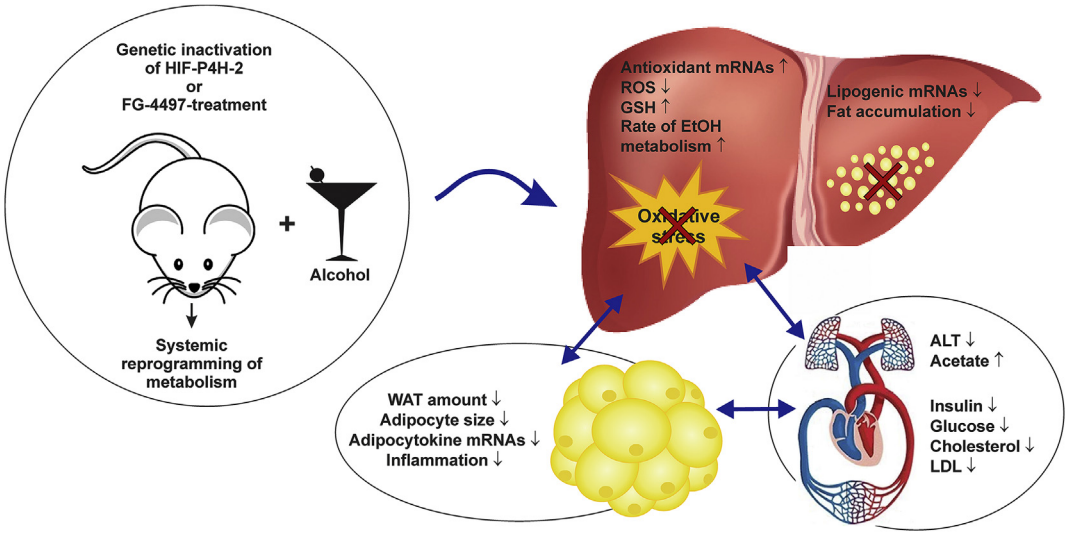

Fig. 6. Schematic for the tissue interplay contributing to protection against AFLD following global activation of the hypoxia response in mice. Abbreviations: ALT, alanine aminotransferase; EtOH, ethanol; GSH, reduced glutathione; ROS, reactive oxygen species; WAT, white adipose tissue.

HIF-P4H-2 inhibition. Also, it is known that the different HIFα paralogues may contribute differently to the outcome [28]. Moreover, as shown here, the interplay between tissues appears important for the protective phenotype (Fig. 6). Restriction of the activation of the hypoxia response to a single tissue is therefore likely to result in different outcome to that obtained in a global setting.

Leptin levels, reflecting the amount of energy stored in adipose tissue, are typically elevated in the presence of inflammation and infection [29]. Serum leptin has also been reported to serve as an independent predictor of the grade of hepatic steatosis in NAFLD [30]. The anti-lipogenic effect of leptin is mediated by a reduction in the level of SREBP1c expression [30]. Our *Hif-p4h-2*$^{gt/gt}$ and WT mice given FG-4497 had reduced adipose tissue and expressed lower amounts of the most abundant adipocytokines [29,30], *Lep* and *Ccl2* mRNAs, whose expression levels associated with a lesser amount of the insulin resistance contributing WAT macrophage crowns, a trend towards reduced steatosis and significantly lower serum ALT levels, respectively (Fig. 6). Altogether, these findings underline the importance of tissue interplay in regulating metabolic health.

Binge drinking of alcohol has been shown to promote hypoxic liver injury in mice and humans through a CYP2E1-HIF1α-dependent apoptosis pathway [22]. Moreover, alcohol has been shown to cause hypoxia and HIF1α stabilization in cells and it has been suggested that HIF1α may have a causative role in AFLD in a hepatocyte-specific setting [21]. Our present data show that ethanol did not stabilize HIF1α or HIF2α in WT primary murine hepatocytes. However, one has to also consider that differences in the obtained data may stem from differences in the ethanol concentrations in the *in vivo* and cellular experiments, and from the more chronic *vs.* acute setting, respectively. However, our data suggest that HIF-P4H-2 inhibition could have generated a HIF-dependent scenario before ethanol administration that can have preconditioned the liver tissue against ethanol-induced liver steatosis and injury. Moreover, HIF-P4H-2 inhibition upregulated the antioxidant HIF-target gene *Gclc* and *Sod2* mRNAs [31,32] in hepatocytes and resulted in higher levels of GSH. High insulin levels have been shown to downregulate ALDH2 catalytic activity [33]. ALDH2 is mediated transcriptionally positively by pVHL, but the mediation is not HIF-dependent [34]. The higher ALDH2 activity and increased serum acetate levels in the *Hif-p4h-2*$^{gt/gt}$ mice must therefore have been mediated by the lower serum insulin levels detected in them. These data further suggest that individuals with metabolic syndrome who suffer from insulin resistance might also have a higher risk of AFLD due to impaired ethanol metabolism.

The data presented here is potentially of very high medical importance, as no targeted therapy is available for AFLD. They suggest that HIF-P4H inhibitors, which are now in the final phase of clinical trials for the treatment of renal anemia [35], could also be considered in the case of AFLD. This would require pharmacokinetic development of the current compounds that are targeted to induce erythropoietin expression to enable them to target specifically the liver and adipose tissue, and perhaps also other tissues, and avoid excess induction of erythropoiesis. Pre-clinical studies have shown that there are additional conditions in which pharmacological HIF-P4H inhibition may be of potential therapeutic value. These include ischemic, infectious and inflammatory diseases [6,28,36,37]. Our data here furthermore suggest that selective HIF-P4H-2 inhibition might be superior in having beneficial effects also on NAFLD, where lipogenesis driven by a surplus energy supply combined with inflammation play major roles.

Authors' contributions

AL, TO, RS, EYD and PK performed the experiments and analyzed the data. DM and VI contributed to the ROS measurements and KMH to histological analyses of the liver. TK put forward suggestions on the experimental design. GW provided FG-4497 and made useful suggestions. JM contributed to generating the *Hif-p4h-2*$^{gt/gt}$ mouse line and participated in the discussions. PK contributed to generating the *Hif-p4h-2*$^{gt/gt}$ mouse line and wrote the paper.

Conflicts of interest

GW is an employee and a shareholder of FibroGen Inc., which develops HIF-P4H inhibitors as potential therapeutics. JM owns equity in the company, which supports research headed by JM.

Acknowledgements

We thank T. Aatsinki, E. Lehtimäki, S. Moilanen and R. Vuento for expert technical assistance.

Appendix A. Supplementary data

Supplementary data to this article can be found online at https://doi.org/10.1016/j.redox.2019.101145.

Financial support

This study was supported by Academy of Finland grants 266719 and 308009 (PK), 296498 (JM), and 296027 (TK), the Academy of Finland Center of Excellence 2012–2017 grant 251314 (JM), and grants from the S. Jusélius Foundation (PK), the Emil Aaltonen Foundation (PK) and the Jane and Aatos Erkko Foundation (PK, TK, JM).

References

[1] R.S. O'Shea, S. Dasarathy, A.J. McCullough, Practice guideline committee of the American association for the study of liver diseases, practice parameters committee of the American college of gastroenterology. Alcoholic liver disease, Hepatology 51 (1) (2010) 307–328.
[2] B. Gao, R. Bataller, Alcoholic liver disease: pathogenesis and new therapeutic targets, Gastroenterology 141 (5) (2011) 1572–1585.
[3] M.R. Lucey, P. Mathurin, T.R. Morgan, Alcoholic hepatitis, N. Engl. J. Med. 360 (26) (2009) 2758–2769.
[4] T.M. Leung, N. Nieto, CYP2E1 and oxidant stress in alcoholic and non-alcoholic fatty liver disease, J. Hepatol. 58 (2) (2013) 395–398.
[5] W.G. Kaelin Jr., P.J. Ratcliffe, Oxygen sensing by metazoans: the central role of the HIF hydroxylase pathway, Mol. Cell. 30 (4) (2008) 393–402.
[6] P. Koivunen, R. Serpi, E.Y. Dimova, Hypoxia-inducible factor prolyl 4-hydroxylase inhibition in cardiometabolic diseases, Pharmacol. Res. 114 (2016) 265–273.
[7] G.L. Semenza, Hypoxia-inducible factors in physiology and medicine, Cell 148 (3) (2012) 399–408.
[8] E. Berra, E. Benizri, A. Ginouves, V. Volmat, D. Roux, J. Pouyssegur, HIF prolyl-hydroxylase 2 is the key oxygen sensor setting low steady-state levels of HIF-1alpha in normoxia, EMBO J. 22 (16) (2003) 4082–4090.
[9] K. Takeda, A. Cowan, G.H. Fong, Essential role for prolyl hydroxylase domain protein 2 in oxygen homeostasis of the adult vascular system, Circulation 116 (7) (2007) 774–781.
[10] K. Takeda, V.C. Ho, H. Takeda, L.J. Duan, A. Nagy, G.H. Fong, Placental but not heart defects are associated with elevated hypoxia-inducible factor alpha levels in mice lacking prolyl hydroxylase domain protein 2, Mol. Cell Biol. 26 (22) (2006) 8336–8346.
[11] Y.A. Minamishima, J. Moslehi, N. Bardeesy, D. Cullen, R.T. Bronson, W.G. Kaelin Jr., Somatic inactivation of the PHD2 prolyl hydroxylase causes polycythemia and congestive heart failure, Blood 111 (6) (2008) 3236–3244.
[12] M. Hirsilä, P. Koivunen, V. Gunzler, K.I. Kivirikko, J. Myllyharju, Characterization of the human prolyl 4-hydroxylases that modify the hypoxia-inducible factor, J. Biol. Chem. 278 (33) (2003) 30772–30780.
[13] C. Ju, S.P. Colgan, H.K. Eltzschig, Hypoxia-inducible factors as molecular targets for liver diseases, J. Mol. Med. (Berl) 94 (6) (2016) 613–627.
[14] L. Rahtu-Korpela, S. Karsikas, S. Hörkkö, R. Blanco Sequeiros, E. Lammentausta, K.A. Mäkelä, K.H. Herzig, et al., HIF prolyl 4-hydroxylase-2 inhibition improves glucose and lipid metabolism and protects against obesity and metabolic dysfunction, Diabetes 63 (10) (2014) 3324–3333.
[15] J. Hyvärinen, I.E. Hassinen, R. Sormunen, J.M. Mäki, K.I. Kivirikko, P. Koivunen, J. Myllyharju, Hearts of hypoxia-inducible factor prolyl 4-hydroxylase-2 hypomorphic mice show protection against acute ischemia-reperfusion injury, J. Biol. Chem. 285 (18) (2010) 13646–13657.
[16] W.T. Friedewald, R.I. Levy, D.S. Fredrickson, Estimation of the concentration of low-density lipoprotein cholesterol in plasma, without use of the preparative ultracentrifuge, Clin. Chem. 18 (6) (1972) 499–502.
[17] P.J. Hissin, R. Hilf, A fluorometric method for determination of oxidized and reduced glutathione in tissues, Anal. Biochem. 74 (1) (1976) 214–226.
[18] A. Konzack, M. Jakupovic, K. Kubaichuk, A. Gorlach, F. Dombrowski, I. Miinalainen, R. Sormunen, et al., Mitochondrial dysfunction due to lack of manganese superoxide dismutase promotes hepatocarcinogenesis, Antioxidants Redox Signal. 23 (14) (2015) 1059–1075.
[19] J.L. Steiner, C.H. Lang, Alcohol, adipose tissue and lipid dysregulation, Biomolecules 7 (1) (2017), https://doi.org/10.3390/biom7010016.
[20] J. Behari, K.G. Sylvester, Role of the wnt/beta-catenin pathway in the pathogenesis of alcoholic liver disease, Curr. Mol. Pharmacol. 10 (3) (2017) 186–194.
[21] B. Nath, I. Levin, T. Csak, J. Petrasek, C. Mueller, K. Kodys, D. Catalano, et al., Hepatocyte-specific hypoxia-inducible factor-1alpha is a determinant of lipid accumulation and liver injury in alcohol-induced steatosis in mice, Hepatology 53 (5) (2011) 1526–1537.
[22] J.W. Yun, M.J. Son, M.A. Abdelmegeed, A. Banerjee, T.R. Morgan, S.H. Yoo, B.J. Song, Binge alcohol promotes hypoxic liver injury through a CYP2E1-HIF-1alpha-dependent apoptosis pathway in mice and humans, Free Radic. Biol. Med. 77 (2014) 183–194.
[23] V.H. Haase, J.N. Glickman, M. Socolovsky, R. Jaenisch, Vascular tumors in livers with targeted inactivation of the von hippel-lindau tumor suppressor, Proc. Natl. Acad. Sci. U. S. A. 98 (4) (2001) 1583–1588.
[24] Y.A. Minamishima, J. Moslehi, R.F. Padera, R.T. Bronson, R. Liao, W.G. Kaelin Jr., A feedback loop involving the Phd3 prolyl hydroxylase tunes the mammalian hypoxic response in vivo, Mol. Cell Biol. 29 (21) (2009) 5729–5741.
[25] E.B. Rankin, J. Rha, M.A. Selak, T.L. Unger, B. Keith, Q. Liu, V.H. Haase, Hypoxia-inducible factor 2 regulates hepatic lipid metabolism, Mol. Cell Biol. 29 (16) (2009) 4527–4538.
[26] C. Xie, T. Yagai, Y. Luo, X. Liang, T. Chen, Q. Wang, D. Sun, et al., Activation of intestinal hypoxia-inducible factor 2alpha during obesity contributes to hepatic steatosis, Nat. Med. 23 (11) (2017) 1298–1308.
[27] R. Kerkelä, S. Karsikas, Z. Szabo, R. Serpi, J. Magga, E. Gao, K. Alitalo, et al., Activation of hypoxia response in endothelial cells contributes to ischemic cardioprotection, Mol. Cell Biol. 33 (16) (2013) 3321–3329.
[28] P. Koivunen, T. Kietzmann, Hypoxia-inducible factor prolyl 4-hydroxylases and metabolism, Trends Mol. Med. 24 (12) (2018) 1021–1035.
[29] N. Iikuni, Q.L. Lam, L. Lu, G. Matarese, A. La Cava, Leptin and inflammation, Curr. Immunol. Rev. 4 (2) (2008) 70–79.
[30] S. Chitturi, G. Farrell, L. Frost, A. Kriketos, R. Lin, C. Fung, C. Liddle, et al., Serum leptin in NASH correlates with hepatic steatosis but not fibrosis: a manifestation of lipotoxicity? Hepatology 36 (2) (2002) 403–409.
[31] H. Lu, D. Samanta, L. Xiang, H. Zhang, H. Hu, I. Chen, J.W. Bullen, et al., Chemotherapy triggers HIF-1-dependent glutathione synthesis and copper chelation that induces the breast cancer stem cell phenotype, Proc. Natl. Acad. Sci. U. S. A. 112 (33) (2015) E4600–E4609.
[32] Y. Oktay, E. Dioum, S. Matsuzaki, K. Ding, L.J. Yan, R.G. Haller, L.I. Szweda, et al., Hypoxia-inducible factor 2alpha regulates expression of the mitochondrial aconitase chaperone protein frataxin, J. Biol. Chem. 282 (16) (2007) 11750–11756.
[33] D.W. Crabb, M.J. Stewart, Q. Xiao, Hormonal and chemical influences on the expression of class 2 aldehyde dehydrogenases in rat H4IIEC3 and human HuH7 hepatoma cells, Alcohol Clin. Exp. Res. 19 (6) (1995) 1414–1419.
[34] Y.H. Gao, Z.X. Wu, L.Q. Xie, C.X. Li, Y.Q. Mao, Y.T. Duan, B. Han, et al., VHL deficiency augments anthracycline sensitivity of clear cell renal cell carcinomas by down-regulating ALDH2, Nat. Commun. 8 (2017) 15337.
[35] A. Besarab, E. Chernyavskaya, I. Motylev, E. Shutov, L.M. Kumbar, K. Gurevich, D.T. Chan, et al., Roxadustat (FG-4592): correction of anemia in incident dialysis patients, J. Am. Soc. Nephrol. 27 (4) (2016) 1225–1233.
[36] H.K. Eltzschig, D.L. Bratton, S.P. Colgan, Targeting hypoxia signalling for the treatment of ischaemic and inflammatory diseases, Nat. Rev. Drug Discov. 13 (11) (2014) 852–869.
[37] C.T. Taylor, G. Doherty, P.G. Fallon, E.P. Cummins, Hypoxia-dependent regulation of inflammatory pathways in immune cells, J. Clin. Invest. 126 (10) (2016) 3716–3724.